

Research



Cite this article: Lohr MJ, Sugerman GP, Kakaletsis S, Lejeune E, Rausch MK. 2022 An introduction to the Ogden model in biomechanics: benefits, implementation tools and limitations. *Phil. Trans. R. Soc. A* **380**: 20210365.
<https://doi.org/10.1098/rsta.2021.0365>

Received: 15 December 2021

Accepted: 14 March 2022

One contribution of 15 to a theme issue 'The Ogden model of rubber mechanics: Fifty years of impact on nonlinear elasticity'.

Subject Areas:

biomedical engineering, materials science, mechanical engineering, biomechanics, mechanics

Keywords:

open data, constitutive modelling, hyperelasticity, brain, blood clot, thrombus

Author for correspondence:

Manuel K. Rausch

e-mail: manuel.rausch@utexas.edu


Electronic supplementary material is available online at <https://doi.org/10.6084/m9.figshare.c.6098644>.

An introduction to the Ogden model in biomechanics: benefits, implementation tools and limitations

Matthew J. Lohr¹, Gabriella P. Sugerman¹,
Sotirios Kakaletsis², Emma Lejeune⁴ and
Manuel K. Rausch^{1,2,3}

¹Department of Biomedical Engineering, ²Department of Aerospace Engineering and Engineering Mechanics, and ³Oden Institute for Computational Engineering and Sciences, University of Texas at Austin, Austin, TX, USA

⁴Department of Mechanical Engineering, Boston University, Boston, MA, USA

 MJL, 0000-0003-3944-6651; GPS, 0000-0001-9904-5257; SK, 0000-0001-9400-9265; MKR, 0000-0003-1337-6472

Constitutive models are important to biomechanics for two key reasons. First, constitutive modelling is an essential component of characterizing tissues' mechanical properties for informing theoretical and computational models of biomechanical systems. Second, constitutive models can be used as a theoretical framework for extracting and comparing key quantities of interest from material characterization experiments. Over the past five decades, the Ogden model has emerged as a popular constitutive model in soft tissue biomechanics with relevance to both informing theoretical and computational models and to comparing material characterization experiments. The goal of this short review is threefold. First, we will discuss the broad relevance of the Ogden model to soft tissue biomechanics and the general characteristics of soft tissues that are suitable for approximating with the Ogden model. Second, we will highlight exemplary uses of the Ogden model in brain tissue, blood clot and other tissues. Finally, we offer a tutorial on fitting the one-term Ogden model to pure shear experimental data via both an analytical approximation of homogeneous deformation and a

finite-element model of the tissue domain. Overall, we anticipate that this short review will serve as a practical introduction to the use of the Ogden model in biomechanics.

This article is part of the theme issue ‘The Ogden model of rubber mechanics: Fifty years of impact on nonlinear elasticity’.

1. Introduction

Ogden introduced in 1972 what we today refer to as the ‘Ogden model’ [1]. At the time, Ogden set out to introduce a material model that was (i) accurate for isotropic, incompressible, ‘rubber-like’ materials under large deformation, and (ii) was more amicable to mathematical analysis than strain invariant-based models. He considered rubber-like materials to be ideally (hyper-)elastic; that is, materials that do not exhibit hysteresis and where the stress is only a function of the strain and in no way a function of its strain history. The strain-energy function he introduced is most commonly quoted as

$$W(\lambda_1, \lambda_2, \lambda_3) = \sum_{i=1}^n \mu_i \frac{[\lambda_1^{\alpha_i} + \lambda_2^{\alpha_i} + \lambda_3^{\alpha_i} - 3]}{\alpha_i}, \quad (1.1)$$

where λ_1 , λ_2 and λ_3 refer to the three principal stretches, and μ_i and α_i are the Ogden material parameters. Please note, though Ogden also introduced a model for compressible materials [2], we will subsequently consider the Ogden model formulated for incompressible materials.

Through the use of the principal stretches as the independent variables, Ogden circumvented the use of the traditional strain invariants I_1 and I_2 , which he felt complicated mathematical analysis [1]. Depending on the choice of n , the material model may be referred to as the one-term Ogden model (for $n = 1$), the two-term Ogden model (for $n = 2$) and so forth. Note that for specific choices of its parameters, the Ogden model recovers both the neo-Hookean model as well as the Mooney–Rivlin model. Consequently, the one-term Ogden model fits experimental data on natural rubber significantly better than the neo-Hookean model and is mathematically simpler than other two-parameter models while fitting data on rubber equally well or better. Given its suitability for rubber-like materials, its simple mathematical form, and its success in fitting experimental data, the Ogden model gained immense popularity culminating in the present special issue in honour of the model’s 50th anniversary.

The model’s popularity has not been limited to rubber-like polymers—the Ogden model is widely used in biomechanics. Specifically, it is frequently used in modelling soft tissues. While soft tissues violate the assumption of perfect elasticity [3,4], treating them as (pseudo-)elastic is often suitable as either a good first approximation to their behaviour, or as an application specific assumption [5,6]. Among soft tissues, those most suited to be approximated using the Ogden model in its original form are isotropic tissues. That is, tissues whose microstructure is sufficiently dispersed so that they may be thought of as random at the macroscale. Commonly, soft tissue such as liver, brain, kidney and blood clot are treated as mechanically isotropic (see more details in §2). By contrast, tissues with well organized, often collagenous, microstructures are typically poorly suited for the unmodified Ogden model as they generally behave anisotropically. Examples for such tissues include skin [7,8], myocardium [9,10], arteries [11,12], skeletal muscle [13,14] and heart valve leaflets [15,16]. In addition, the Ogden model may be well suited for modelling collagenous tissues whose *in vivo* loading is primarily axial and thus can be analysed in one dimension. Examples of such tissues include tendons [17], ligaments [18] and chordae tendineae [19].

The objective of this article is threefold. First, our goal is to introduce the Ogden model to those readers that are unfamiliar with it, especially those in the biomechanics community. We will focus on the effect and interpretation of its parameters and explain what makes the Ogden model particularly suitable to modelling certain classes of soft biological tissues. Second, our goal is to review the use of the Ogden model within biomechanics and discuss

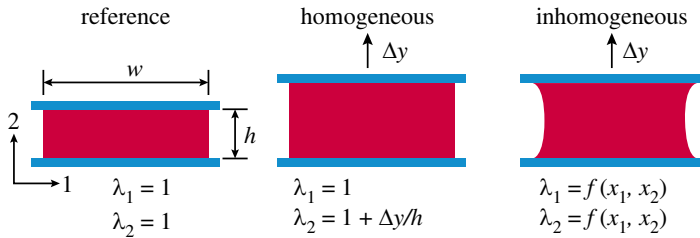


Figure 1. Pure shear as an idealized (homogeneous) and inhomogeneous problem, i.e. the deformation field is a function of the spatial coordinates. Note, pure shear specimens are typically designed with a large width (w) to height (h) ratio such that the deformed width may be considered unchanged, while the thickness may change to preserve volume. (Online version in colour.)

its suitability to specific tissue types. Lastly, our goal is to ease the adoption of the Ogden model by providing practical instructions to its implementation, use and calibration. In this work, we will specifically emphasize the one-term Ogden model. The reasons are as follows: (i) with our objectives being primarily introductory, the one-term model lends itself to simple notation, implementation, and interpretation; (ii) the use of only two parameters—one associated with a material's stiffness, the other with a material's degree of nonlinearity—lends itself (at least theoretically) to quantitative comparisons between tissues in the sense of biomechanical phenotyping [20]. That is, tissues' biomechanical phenotype can be compared statistically by comparing their respective parameters. With this context in mind, the one-term Ogden model reads as

$$W(\lambda_1, \lambda_2, \lambda_3) = \frac{\mu[\lambda_1^\alpha + \lambda_2^\alpha + \lambda_3^\alpha - 3]}{\alpha}. \quad (1.2)$$

Note, in the original work, Ogden noted that the conventional shear modulus may be expressed in terms of μ_i and α_i through the identity $2\mu_0 = \sum \mu_i \alpha_i$ leading to an alternative equation in terms of μ_0 rather than μ . Because the conventional shear modulus is easy to interpret, we too choose this form, written as

$$W(\lambda_1, \lambda_2, \lambda_3) = \frac{2\mu_0[\lambda_1^\alpha + \lambda_2^\alpha + \lambda_3^\alpha - 3]}{\alpha^2}. \quad (1.3)$$

2. The Ogden model in biomechanics

(a) Model suitability and sensitivity

The Ogden model is best suited to represent isotropic materials; that is, materials whose properties are not direction dependent. These materials can be sufficiently characterized with relatively simple test modes such as uniaxial tensile and compression testing, simple shear testing and pure shear testing; albeit, more than one test mode is usually needed to identify unique parameters to the Ogden model [21,22]. In fact, in §3, we will introduce data from a pure shear test on blood clot as an example dataset. Thus, in this current section, we will briefly revisit the kinematic assumptions underlying the idealized—i.e. homogeneous—pure shear testing mode and the corresponding expression of stress, see figure 1. Additionally, for illustrative purposes below, we will use the homogeneous pure shear test to showcase the (one-term) Ogden model's sensitivity to its parameters, and highlight the model's particular suitability for representing soft isotropic biological tissue. However, note that in reality the pure shear testing mode leads to an inhomogeneous problem that may require approximation through computational rather than analytical approaches. We will therefore discuss approaches to material property characterization based on both the homogeneous and the inhomogeneous assumptions in §3. Also, for those readers that are unfamiliar with the pure shear deformation, we provide one (possible) explanation for its peculiar name in the electronic supplementary material.

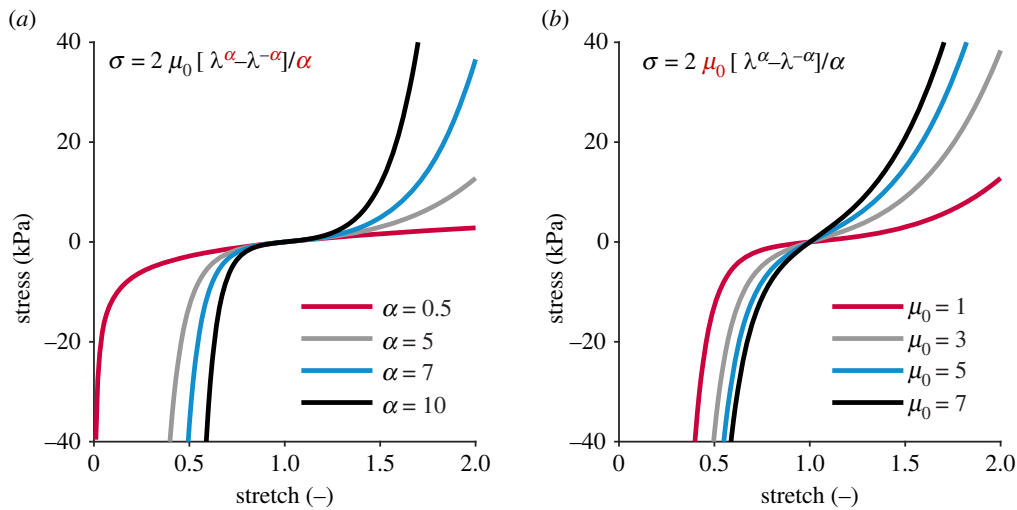


Figure 2. (One-term) Ogden model response to pure shear. (a) Sensitivity to the 'nonlinearity' parameter α with $\mu_0 = 1$. (b) Sensitivity to the conventional shear modulus μ_0 with $\alpha = 5$. (Online version in colour.)

Briefly, under the assumptions of homogeneity and incompressibility, the deformation gradient for pure shear generally reads $\mathbf{F} = \text{diag}(1, \lambda, 1/\lambda)$, where \mathbf{F} is the deformation gradient and λ is the stretch in the loading direction, see figure 1. Given the expression for the Cauchy stress $\sigma_i = \lambda_i \partial W / \partial \lambda_i - p$, we can solve for the Lagrange multiplier p under the assumption of traction-free lateral boundaries to find

$$\sigma = \frac{2\mu_0[\lambda^\alpha - \lambda^{-\alpha}]}{\alpha}. \quad (2.1)$$

Here, we made use of the incompressibility assumption, which dictates that $\lambda_1 \lambda_2 \lambda_3 = 1$ and we replaced λ_2 and σ_2 with λ and σ , respectively. Figure 2 illustrates the one-term Ogden model's predictions of pure shear and the model's sensitivity to the parameters α and μ_0 . In detail, figure 2a illustrates the influence of what is often referred to as the 'nonlinearity parameter' α . Focusing first on the tensile response, it becomes apparent that for $\alpha = 0.5$ the Ogden model predicts strain-softening behaviour. That is, the predicted material stiffness (i.e. slope to the stress-stretch curve) decreases with increasing strain. In fact, the Ogden model predicts strain-softening behaviour for any $|\alpha| < 1$. On the other hand, for $|\alpha| > 1$, the Ogden model predicts strain-stiffening behaviour under tensile loading as seen for $\alpha = 5, 7, 10$. It is this latter property that makes the Ogden model suitable to soft tissues, many of which exhibit strain stiffening due to their fibrous, semi-flexible, biopolymeric microstructure [23]. Figure 2b illustrates the influence of the conventional shear modulus μ_0 . As one would expect of the shear modulus, it scales the material response. That is, increasing μ_0 leads to an increase in overall stiffness. Note under compression the Ogden model is always strain stiffening. Consequently, a nonlinearity parameter $|\alpha| < 1$ not only leads to strain softening under tension, but also to tension-compression nonlinearity. It is this latter property that has led others to term α the 'tension-compression nonlinearity parameter'.

Note, one drawback of using pure shear as an example loading mode is that its expression for stress is symmetric in the sign of α . Thus, positive and negative α s yield the same result. This is not generally true. For example, the stress under uniaxial extension reads

$$\sigma = \frac{2\mu_0 [\lambda^\alpha - \lambda^{-\alpha/2}]}{\alpha}. \quad (2.2)$$

Thereby, a sign change of α modulates whether the material stiffens at a higher rate under tension, or compression (more on this limitation in §4).

(b) Prior uses of the Ogden model in biomechanics: from head to toe

Among the many applications of the Ogden model in biomechanics, it has found the most widespread use within the brain biomechanics community [24]. For modelling brain tissue, the Ogden model is used in its one-term, two-term, three-term or even higher term form [25] and informed through simple shear experiments [26], compression experiments [27–29], uniaxial tensile testing [30–32], indentation experiments [33] or a combination thereof [34]. For the one-term Ogden model, reports on the nonlinearity parameter α and the shear modulus μ_0 vary widely. Such differences may stem from inter-subject and inter-species variability, differences in test modes and protocols, different storage and mounting procedures etc. [35]. However, even within the same study α for brain tissue has been reported in the range of -82.9 to 48.2 [20]. Thus, wide variety in reported α is likely not due to physiological factors, but rather fitting issues and model-inherent limitations. In fact, it was previously suggested that the Ogden model is relatively insensitive to α under some loading conditions which partially explains its large variability among studies [36]. Additionally, as Budday *et al.* pointed out, incomplete choice of loading modes may fail to capture the full material response of brain tissues—and other tissues—and thus lead to inappropriate fitting of the α parameter [20]. Others have noted this challenge before and suggested using multiple test modes to inform α [21,22]. Alternatively, Yeoh proposed to fix a reasonable value of α during the fitting procedure or to impose reasonable bounds during constrained fitting [36]. By contrast, the shear modulus μ_0 is relatively conserved across studies, implying that it has more value as a measure of a tissue's biomechanical phenotype [20,30,33]. As a brief summary of this extensive previous work on modelling brain tissue with the Ogden model, 'the classical Ogden model is a well-suited phenomenological model to characterize the time-independent behaviour of the brain tissue' as stated by de Rooij *et al.* [37]. Although, even beyond the quasi-static approximation of brain tissues, the Ogden model is of value. To capture the time-dependent behaviour of brain tissue, many applications have previously coupled the Ogden model to either a poroelastic or a viscoelastic formulation [38,39]. Regardless of the specific choice of the model, whether by itself, extended through time-dependent terms, or augmented with anisotropic terms [40], the Ogden model has shown to be a versatile and appropriate model for capturing the mechanics of brain tissue. Beyond modelling brain tissue, the Ogden model has also been used for many other soft tissues. For example, it has also been used to model blood clot. Similar to brain tissue, the Ogden model for blood clot has been informed via simple shear experiments [41], pure shear experiments [42], compression experiments [43] and under mixed modes [44]. In fact, our case study in §3 is comprised of pure shear experimental data of *in vitro* blood clot. In addition to brain tissue and blood clot, the Ogden model has also been used to model liver tissue (including its capsule) [45]. Similarly to brain tissue and blood clot, the Ogden model for the liver has been informed via uniaxial extension [46,47], compression [48] and indentation [49]. Also similarly to the applications described above, the Ogden model for liver has been applied in its one-term form [50] and multi-term form [49], and has been modified through inclusion of viscoelastic extensions [51,52] and via logarithmic and exponential terms [53]. Liver, spleen and kidney have also been modelled via Ogden's strain-energy function [54,55]. Finally, the Ogden model has been widely popular in foot biomechanics, where it has been used extensively to model plantar soft tissue [56–61]. In summary, the Ogden model has been used to model many of our bodies' most important tissues, ranging all the way from head to toe.

3. A case study

As part of our practical guide to the Ogden model, we collected an example experimental dataset which we then used to demonstrate two differing approaches to calibrating the Ogden material parameters. While we limit ourselves again to the one-term Ogden model for simplicity, both

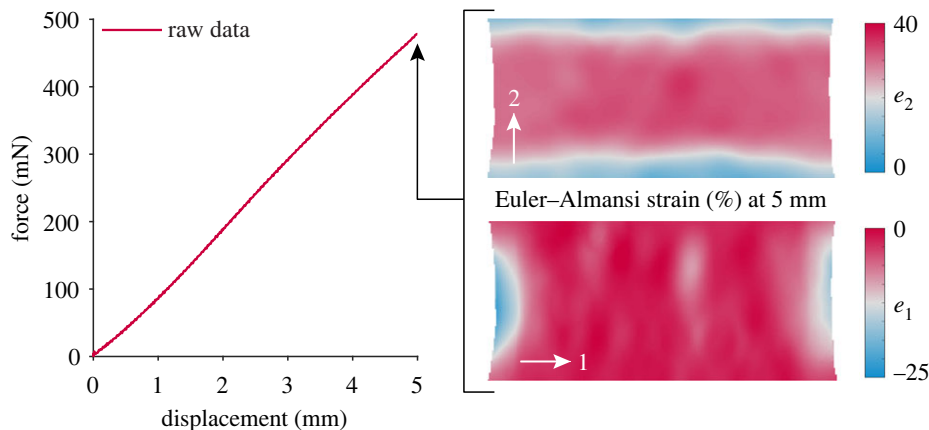


Figure 3. Example blood clot dataset. Force–displacement curve as measured under pure shear and the corresponding digital image correlation-based visualization of the Euler–Almansi strain. (Online version in colour.)

approaches are generally applicable to multiple terms with only minor changes to the example code provided with this manuscript. Please also note that we do not discuss the numerical implementation of the Ogden model within the finite-element framework, as the Ogden model is widely implemented in both commercial [36] and open source [62] finite-element codes. However, we refer those readers interested in the implementation of the Ogden model to a wonderful resource by Connolly *et al.* [63].

(a) The pure shear dataset

For the purpose of this guide, we collected pure shear data on blood clot. We previously described the blood coagulation methods and experimental methods in detail [64]. Thus, we only briefly summarize them here. First, we coagulated fresh bovine blood into a three-dimensional printed mould of a pure shear geometry that spanned 40 mm by 10 mm by 3 mm in one, two and three dimensions, respectively. We speckled the sample with sand for full-field digital image correlation (DIC), and mounted the sample in our uniaxial tensile tester (Instron 5943, 10 N load cell). After mounting, we extended the upper mount at a rate of 0.5 mm s^{-1} until the sample failed. During testing, we recorded the measured force, time and the displacement. Simultaneously, we imaged the sample at a rate of 3 Hz. After concluding our experiments, we used the open source DIC software NCORR (www.ncorr.com) to compute the Euler–Almansi strain of our sample [65]. Figure 3 shows the raw data up until a displacement of 5 mm. Please note that the raw data file provided with our work contains the full dataset up until failure, which we are not displaying or fitting here. Figure 3 also shows the DIC-derived Euler–Almansi strain map in the one- and two-directions at a displacement of 5 mm. From these images, it is evident that the deformation field is not homogeneous, i.e. the strain field is a function of the spatial coordinates x_1 and x_2 . Nevertheless, note that the plane strain assumption in direction 1 (i.e. the pure shear deformation mode) is satisfied throughout most of the sample width, which motivates the homogeneous description in the next section.

(b) Homogeneous pure shear

The advantage of assuming that the pure shear experiment leads to a homogeneous deformation field lies in the existence of a simple, closed-form solution. See §2 to revisit this solution. The assumption of homogeneity is based on the notion that a large sample width relative to sample height leads to negligible stretch in the one-direction. As shown in figure 3, this is clearly not the case for our example dataset. Nonetheless, the assumption of homogeneity

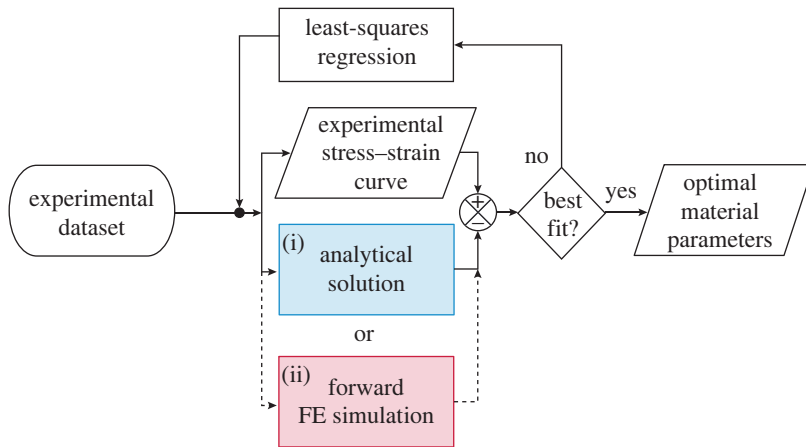


Figure 4. Schematic of the pipeline for fitting the Ogden model parameters to an experimental dataset. In §3b, we provide details on (i) the analytical solution and in §3c we provide details on the forward finite-element (FE) simulation (ii). (Online version in colour.)

can be a good first approximation. Figure 4(i) shows the pipeline for the inverse parameter identification for the Ogden material model based on the analytical solution to the homogeneous pure shear problem. This pipeline is very general and applicable not just to the Ogden model, but to other material models and mechanical test mode combinations. In fact, this pipeline is also applicable to the problem of heterogeneous pure shear through replacing the analytical solution with a finite-element approach, see figure 4(ii). We and others have used this or similar approaches extensively for the purpose of identifying material parameters for soft tissues [66,67]. In short, we use a least-squares solver to minimize an objective function that penalizes the difference between our experimental force–displacement—or, equivalently—stress–stretch data and our analytically predicted data. By iteratively improving each parameter guess, the solver subsequently minimizes the error until convergence is achieved and the final optimal parameter set has been identified. We implemented this pipeline in a Jupyter Notebook that is openly available with our work and can be freely adapted by the reader to their specific data. Based on this pipeline, we found the optimal Ogden parameters for our dataset to be $\alpha = 4.28$ and $\mu_0 = 2.38$ kPa. The resulting fit between our experimental data and our analytical predictions is excellent with a root mean square error (RMSE) of 9.92 mN, see figure 5. The actual parameter values reflect those reported for blood clot by our own laboratory and by others very well [41].

(c) Inhomogeneous pure shear

From the DIC-based strain visualization in figure 3, we see that our pure shear experiments did not lead to a perfectly homogeneous deformation field. Therefore, the assumptions underlying our analytical solutions are, to some extent, inaccurate. In contrast to our analytical solution, a finite-element-based solution to the boundary value problem can account for such inhomogeneities and may therefore yield more accurate estimates of the Ogden parameters from our example pure shear experiment. To introduce how to conduct such analysis and contrast the results to the approach in §3b, we use the same inverse pipeline schematically illustrated in figure 4, and replace the analytical solution with the solution of a finite-element forward simulation. For the simulation itself, we use the nonlinear finite-element solver FEBio (www.febio.org) [62]. Within FEBio, we define the sample geometry to mimic our experimental sample, but take advantage of symmetry and only model one-eighth of the geometry, see figure 6a. We discretize the geometry using 9600 linear hexahedral elements (bricks). To account for near incompressibility, we use a (H1P0) hybrid element formulation and choose a bulk modulus of

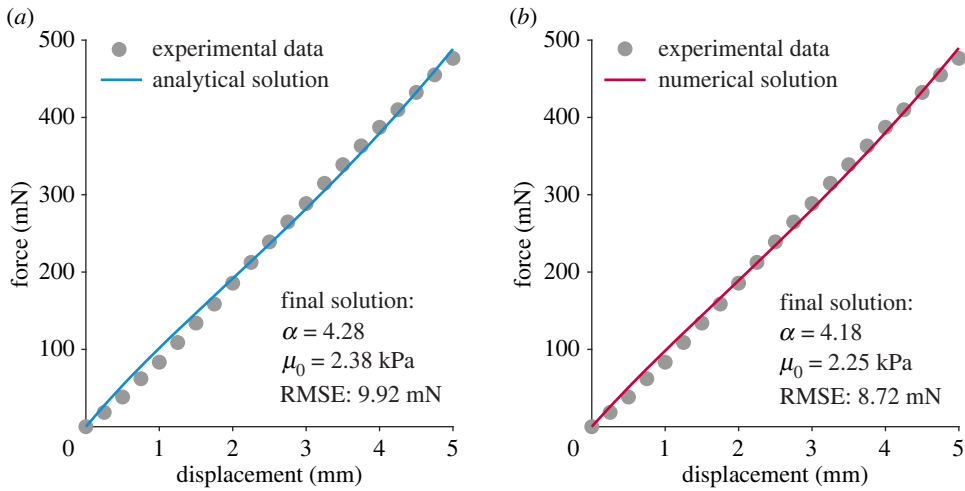


Figure 5. Ogden material parameter identification. (a) Curve fit between the analytical solution of the homogeneous pure shear problem and our example dataset. (b) Curve fit between the numerical solution of the inhomogeneous pure shear problem and our example dataset. RMSE, root mean square error. (Online version in colour.)

1 GPa (approximately five orders of magnitude higher than our shear modulus) [62]. To mimic our experiments, we attach a rigid body to the top surface of our sample and displace this rigid body by 2.5 mm (note that given the symmetry condition this is equivalent to the experimental displacement of 5.0 mm). Subsequently, we repeatedly perform this simulation with consecutively improved guesses for the two Ogden parameters α and μ_0 until reaching the same convergence criteria as for the homogeneous pure shear problem. Figure 6*b,c* shows the finite-element solution for our converged parameter set. We can clearly see that the strain fields in both the one-direction and the two-direction are inhomogeneous, albeit only slightly so in the one-direction. Additionally, we see that the results compare well with our experimental results from figure 3. We implemented this pipeline in a Jupyter Notebook that is openly available with our work and can be freely adapted by the reader to their specific data. Based on this pipeline, we found the optimal Ogden parameters for our dataset to be $\alpha = 4.18$ and $\mu_0 = 2.25$ kPa. The resulting fit between our experimental data and our numerical predictions is also excellent with a RMSE of 8.72 mN, see figure 5. It may be noted here that the numerical solution yields slightly different parameter values from those obtained through the analytical approach. Additionally, the RMSE is slightly smaller. Together these results indicate that the analytical solution does indeed give a very good approximation to the problem, but yields slightly worse fits. This result is well aligned with our DIC-based findings that the actual deformation field was homogeneous across most of the sample, see figure 3 for reference.

(d) Notes on the parameter fitting tutorial

In figure 4, we illustrate the basic pipeline for computing Ogden model material parameters from experimental data. The key components to this pipeline are: (i) the input experimental data, (ii) the implemented Ogden model and (iii) the least-squares regression solver. As described in §3b and 3c, the Ogden model can take the form of either an analytical solution or a finite-element analysis simulation. Under ‘Data Accessibility’, we provide a link to our Python Jupyter Notebook [68] tutorial on implementing this pipeline. The tutorial begins with basic importing and visualization of the experimental force–displacement data. The second part of the tutorial demonstrates how to implement the pure shear analytical solution for the one-term Ogden model and solve for optimal parameters using the `scipy` function ‘`optimize.curvefit`’ [69]. Because we bound the parameter

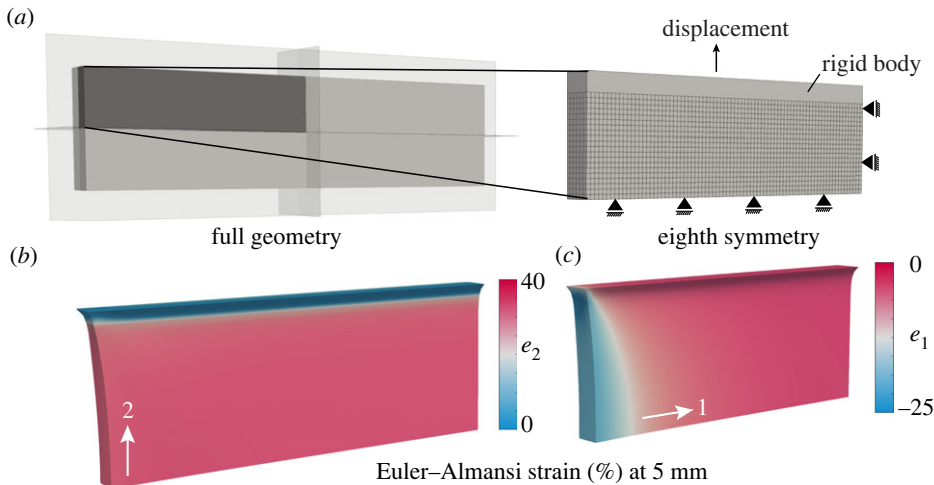


Figure 6. Numerical model and simulation results for the inhomogeneous pure shear problem. (a) We took advantage of pure shear's symmetry and modelled only one-eighth of the full sample geometry. (b) Euler–Almansi strain at 5 mm of displacement in the two-direction. (c) Euler–Almansi strain at 5 mm of displacement in the one-direction. (Online version in colour.)

space for α and μ_0 ($-100 < \alpha < 100$ and $0 < \mu_0 < \infty$ kPa), optimization is performed with the Trust Region Reflective algorithm [70]. Please note that we tested our inverse identification against multiple initial guesses to ensure that we found non-local minima within our parameter space. We recommend users do the same when extending our pipeline to other scenarios. The third part of the tutorial demonstrates how to call the finite element analysis software FEBio [62] from a Python script and solve for optimal parameters using the same approach as above. For both strategies, we also provide code to visualize results. This tutorial provides a concise starting point for soft tissue material characterization with the Ogden model. One final note to the reader: as mentioned earlier in this text, ensuring uniqueness of material parameters may require using more than one test mode. For example, Ogden *et al.* suggested combining uniaxial tensile testing with biaxial testing [22]. Similarly, Latorre *et al.* suggested using uniaxial tensile tests with compression tests [21]. Fortunately, our pipeline can be easily extended to this end. To do so, our fitting pipeline can be extended by including the least-square errors to both tests in the objective function.

4. Limitations and concerns

No model is perfect, and the Ogden model is no exception. We have previously mentioned that the Ogden model appears relatively insensitive to α under some loading conditions. This concern has been voiced by others [36]. Specifically, in the context of biomechanical applications, this implies that α is likely not a good parameter by which to compare materials. Instead, for biomechanical phenotyping purposes, the conventional shear modulus μ_0 is often the better choice. We have also mentioned previously that the Ogden parameter α simultaneously controls the tension-compression nonlinearity, the degree of which cannot be separately controlled, and the degree of nonlinearity. This can be a severe limitation, especially when only tension or compression data are available and the actual tension-compression nonlinearity is unknown. Fortunately, Moerman *et al.* have introduced an extension to the Ogden model, through which the tension-compression nonlinearity can be controlled [71], thus overcoming this limitation of the Ogden model. Additionally, it has previously been pointed out that the Ogden model is purely phenomenological. Interestingly, Ehret has addressed this concern and shown that the Ogden material can be expressed in terms of physical constants characterizing the polymer chain and network [72]. Thereby, Ehret challenges the notion that the Ogden model is entirely phenomenological.

5. Conclusion

In our work, we discussed the broad relevance and success of the Ogden model in soft tissue biomechanics and the general characteristics of soft tissues that are suitably approximated by the Ogden model. Additionally, we highlighted the exemplary use of the Ogden model in brain tissue, blood clot and other tissues. Finally, we offered a tutorial on fitting the (one-term) Ogden model to pure shear experimental data via both an analytical approximation of homogeneous deformation and a finite-element model of the tissue domain. Thereby, we believe, we achieved our goals and provided readers a practical, yet informative introduction to the Ogden model in biomechanics.

Data accessibility. The data and code necessary to reproduce all figures in this manuscript are available on our GitHub page <https://github.com/ejejeune11/fitting-one-term-ogden-model>. In addition, the GitHub page contains a Jupyter Notebook Tutorial for fitting a one-term Ogden model to pure shear experimental data. The data are provided in the electronic supplementary material [73].

Authors' contributions. M.J.L.: formal analysis, investigation, methodology, software, writing—original draft; G.P.S.: data curation, investigation, methodology, writing—original draft; S.K.: data curation, formal analysis, software, visualization, writing—original draft; E.L.: conceptualization, data curation, formal analysis, investigation, methodology, resources, software, validation, visualization, writing—original draft; M.K.R.: conceptualization, data curation, formal analysis, funding acquisition, investigation, methodology, project administration, resources, software, supervision, validation, visualization, writing—original draft.

All authors gave final approval for publication and agreed to be held accountable for the work performed therein.

Conflict of interest declaration. Dr Rausch has a speaking agreement with Edwards Lifesciences. No other authors have potential conflicts to report.

Funding. This work was partially funded through the NSF grant nos. 2046148, 2105175 and 2127925 and ONR grant no. N00014-22-1-2073. The opinions, findings, and conclusions, or recommendations expressed are those of the authors and do not necessarily reflect the views of the NSF. Additionally, this work was supported through the Williams Faculty Excellence Fund.

Acknowledgements. Many thanks to the organizers of this special issue for the invitation and their editorial support.

References

- Ogden RW. 1972 Large deformation isotropic elasticity—on the correlation of theory and experiment for incompressible rubberlike solids. *Proc. R. Soc. Lond. A* **326**, 565–584. (doi:10.1098/rspa.1972.0026)
- Ogden RW. 1972 Large deformation isotropic elasticity—on the correlation of theory and experiment for compressible rubberlike solids. *Proc. R. Soc. Lond. A* **328**, 567–583. (doi:10.1098/rspa.1972.0096)
- Haslach HW. 2005 Nonlinear viscoelastic, thermodynamically consistent, models for biological soft tissue. *Biomech. Model. Mechanobiol.* **3**, 172–189. (doi:10.1007/s10237-004-0055-6)
- Weickenmeier J, Jabareen M. 2014 Elastic–viscoplastic modeling of soft biological tissues using a mixed finite element formulation based on the relative deformation gradient. *Int. J. Numer. Methods Biomed. Eng.* **30**, 1238–1262. (doi:10.1002/cnm.2654)
- Fung Y, Fronek K, Patitucci P. 1979 Pseudoelasticity of arteries and the choice of its mathematical expression. *Am. J. Physiol.-Heart Circ. Physiol.* **237**, H620–H631. (doi:10.1152/ajpheart.1979.237.5.H620)
- Tong P, Fung YC. 1976 The stress-strain relationship for the skin. *J. Biomech.* **9**, 649–657. (doi:10.1016/0021-9290(76)90107-X)
- Tepole AB, Gosain AK, Kuhl E. 2012 Stretching skin: the physiological limit and beyond. *Int. J. Non-Linear Mech.* **47**, 938–949. (doi:10.1016/j.ijnonlinmec.2011.07.006)
- Meador WD, Sugeran GP, Story HM, Seifert AW, Bersi MR, Tepole AB, Rausch MK. 2020 The regional-dependent biaxial behavior of young and aged mouse skin: a detailed histomechanical characterization, residual strain analysis, and constitutive model. *Acta Biomater.* **101**, 403–413. (doi:10.1016/j.actbio.2019.10.020)

9. Sommer G, Schriefl AJ, Andrä M, Sacherer M, Viertler C, Wolinski H, Holzapfel GA. 2015 Biomechanical properties and microstructure of human ventricular myocardium. *Acta Biomater.* **24**, 172–192. (doi:10.1016/j.actbio.2015.06.031)
10. Kakaletsis S, Meador WD, Mathur M, Sugerman GP, Jazwiec T, Malinowski M, Lejeune E, Timek TA, Rausch MK. 2021 Right ventricular myocardial mechanics: multi-modal deformation, microstructure, modeling, and comparison to the left ventricle. *Acta Biomater.* **123**, 154–166. (doi:10.1016/j.actbio.2020.12.006)
11. Wagenseil JE, Mecham RP. 2009 Vascular extracellular matrix and arterial mechanics. *Physiol. Rev.* **89**, 957–989. (doi:10.1152/physrev.00041.2008)
12. Bersi MR, Bellini C, Di Achille P, Humphrey JD, Genovese K, Avril S. 2016 Novel methodology for characterizing regional variations in the material properties of murine aortas. *J. Biomech. Eng.* **138**, 071005. (doi:10.1115/1.4033674)
13. Ehret AE, Böl M, Itskov M. 2011 A continuum constitutive model for the active behaviour of skeletal muscle. *J. Mech. Phys. Solids* **59**, 625–636. (doi:10.1016/j.jmps.2010.12.008)
14. Takaza M, Moerman KM, Gindre J, Lyons G, Simms CK. 2013 The anisotropic mechanical behaviour of passive skeletal muscle tissue subjected to large tensile strain. *J. Mech. Behav. Biomed. Mater.* **17**, 209–220. (doi:10.1016/j.jmbbm.2012.09.001)
15. Meador WD, Mathur M, Sugerman GP, Jazwiec T, Malinowski M, Bersi MR, Timek TA, Rausch MK. 2020 A detailed mechanical and microstructural analysis of ovine tricuspid valve leaflets. *Acta Biomater.* **102**, 100–113. (doi:10.1016/j.actbio.2019.11.039)
16. Ross CJ *et al.* 2021 Effects of enzyme-based removal of collagen and elastin constituents on the biaxial mechanical responses of porcine atrioventricular heart valve anterior leaflets. *Acta Biomater.* **135**, 425–440. (doi:10.1016/j.actbio.2021.08.043)
17. Cheng T, Gan RZ. 2008 Experimental measurement and modeling analysis on mechanical properties of tensor tympani tendon. *Med. Eng. Phys.* **30**, 358–366. (doi:10.1016/j.medengphy.2007.04.005)
18. Cheng T, Gan RZ. 2008 Mechanical properties of anterior malleolar ligament from experimental measurement and material modeling analysis. *Biomech. Model. Mechanobiol.* **7**, 387–394. (doi:10.1007/s10237-007-0094-x)
19. Smith K *et al.* 2021 Tricuspid chordae tendineae mechanics: insertion site, leaflet, and size-specific analysis and constitutive modelling. *Exp. Mech.* **61**, 19–29. (doi:10.1007/s11340-020-00594-5)
20. Budday S *et al.* 2017 Mechanical characterization of human brain tissue. *Acta Biomater.* **48**, 319–340. (doi:10.1016/j.actbio.2016.10.036)
21. Latorre M, De Rosa E, Montáns FJ. 2017 Understanding the need of the compression branch to characterize hyperelastic materials. *Int. J. Non-Linear Mech.* **89**, 14–24. (doi:10.1016/j.ijnonlinmec.2016.11.005)
22. Ogden RW, Saccomandi G, Sgura I. 2004 Fitting hyperelastic models to experimental data. *Comput. Mech.* **34**, 484–502. (doi:10.1007/s00466-004-0593-y)
23. Motte S, Kaufman LJ. 2013 Strain stiffening in collagen I networks. *Biopolymers* **99**, 35–46. (doi:10.1002/bip.22133)
24. Mihai LA, Budday S, Holzapfel GA, Kuhl E, Goriely A. 2017 A family of hyperelastic models for human brain tissue. *J. Mech. Phys. Solids* **106**, 60–79. (doi:10.1016/j.jmps.2017.05.015)
25. Mihai LA, Chin L, Janmey PA, Goriely A. 2015 A comparison of hyperelastic constitutive models applicable to brain and fat tissues. *J. R. Soc. Interface* **12**, 20150486. (doi:10.1098/rsif.2015.0486)
26. Prange MT, Margulies SS. 2002 Regional, directional, and age-dependent properties of the brain undergoing large deformation. *J. Biomech. Eng.* **124**, 244–252. (doi:10.1115/1.1449907)
27. Kohandel M, Sivaloganathan S, Tenti G, Drake J. 2006 The constitutive properties of the brain parenchyma: Part 1. Strain energy approach. *Med. Eng. Phys.* **28**, 449–454. (doi:10.1016/j.medengphy.2005.01.005)
28. Rashid B, Destrade M, Gilchrist MD. 2012 Mechanical characterization of brain tissue in compression at dynamic strain rates. *J. Mech. Behav. Biomed. Mater.* **10**, 23–38. (doi:10.1016/j.jmbbm.2012.01.022)
29. Laksari K, Shafieian M, Darvish K. 2012 Constitutive model for brain tissue under finite compression. *J. Biomech.* **45**, 642–646. (doi:10.1016/j.jbiomech.2011.12.023)
30. Miller K, Chinzei K. 2002 Mechanical properties of brain tissue in tension. *J. Biomech.* **35**, 483–490. (doi:10.1016/S0021-9290(01)00234-2)

31. Rashid B, Destrade M, Gilchrist MD. 2012 Inhomogeneous deformation of brain tissue during tension tests. *Comput. Mater. Sci.* **64**, 295–300. (doi:10.1016/j.commatsci.2012.05.030)
32. Rashid B, Destrade M, Gilchrist MD. 2014 Mechanical characterization of brain tissue in tension at dynamic strain rates. *J. Mech. Behav. Biomed. Mater.* **33**, 43–54. (doi:10.1016/j.jmbbm.2012.07.015)
33. Kaster T, Sack I, Samani A. 2011 Measurement of the hyperelastic properties of *ex vivo* brain tissue slices. *J. Biomech.* **44**, 1158–1163. (doi:10.1016/j.jbiomech.2011.01.019)
34. Moran R, Smith JH, García JJ. 2014 Fitted hyperelastic parameters for human brain tissue from reported tension, compression, and shear tests. *J. Biomech.* **47**, 3762–3766. (doi:10.1016/j.jbiomech.2014.09.030)
35. Prange MT, Meaney DF, Margulies SS. 2000 Defining brain mechanical properties: effects of region, direction, and species. *Stapp Car Crash J.* **44**, 205–213. (doi:10.4271/2000-01-sc15)
36. Yeoh O. 1997 On the Ogden strain-energy function. *Rubber Chem. Technol.* **70**, 175–182. (doi:10.5254/1.3538422)
37. de Rooij R, Kuhl E. 2016 Constitutive modeling of brain tissue: current perspectives. *Appl. Mech. Rev.* **68**, 010801. (doi:10.1115/1.4032436)
38. Budday S, Sommer G, Holzapfel G, Steinmann P, Kuhl E. 2017 Viscoelastic parameter identification of human brain tissue. *J. Mech. Behav. Biomed. Mater.* **74**, 463–476. (doi:10.1016/j.jmbbm.2017.07.014)
39. Budday S, Sommer G, Haybaeck J, Steinmann P, Holzapfel GA, Kuhl E. 2017 Rheological characterization of human brain tissue. *Acta Biomater.* **60**, 315–329. (doi:10.1016/j.actbio.2017.06.024)
40. Velardi F, Fraternali F, Angelillo M. 2006 Anisotropic constitutive equations and experimental tensile behavior of brain tissue. *Biomech. Model. Mechanobiol.* **5**, 53–61. (doi:10.1007/s10237-005-0007-9)
41. Sugerman GP, Kakaletsis S, Thakkar P, Chokshi A, Parekh SH, Rausch MK. 2021 A whole blood thrombus mimic: constitutive behavior under simple shear. *J. Mech. Behav. Biomed. Mater.* **115**, 104216. (doi:10.1016/j.jmbbm.2020.104216)
42. Rausch MK, Sugerman GP, Kakaletsis S, Dortdivanlioglu B. 2021 Hyper-viscoelastic damage modeling of whole blood clot under large deformation. *Biomech. Model. Mechanobiol.* **20**, 1–13. (doi:10.1007/s10237-021-01467-z)
43. Fereidoonzhad B, Moerman KM, Johnson S, McCarthy R, McGarry PJ. 2021 A new compressible hyperelastic model for the multi-axial deformation of blood clot occlusions in vessels. *Biomech. Model. Mechanobiol.* **20**, 1–19. (doi:10.1007/s10237-021-01446-4)
44. Fereidoonzhad B, Dwivedi A, Johnson S, McCarthy R, McGarry P. 2021 Blood clot fracture properties are dependent on red blood cell and fibrin content. *Acta Biomater.* **127**, 213–228. (doi:10.1016/j.actbio.2021.03.052)
45. Umale S, Chatelin S, Bourdet N, Deck C, Diana M, Dhumane P, Soler L, Marescaux J, Willinger R. 2011 Experimental *in vitro* mechanical characterization of porcine Glisson's capsule and hepatic veins. *J. Biomech.* **44**, 1678–1683. (doi:10.1016/j.jbiomech.2011.03.029)
46. Lu YC, Kemper AR, Untaroiu CD. 2014 Effect of storage on tensile material properties of bovine liver. *J. Mech. Behav. Biomed. Mater.* **29**, 339–349. (doi:10.1016/j.jmbbm.2013.09.022)
47. Untaroiu CD, Lu YC. 2013 Material characterization of liver parenchyma using specimen-specific finite element models. *J. Mech. Behav. Biomed. Mater.* **26**, 11–22. (doi:10.1016/j.jmbbm.2013.05.013)
48. Hu T, Desai JP. 2004 Characterization of soft-tissue material properties: large deformation analysis. In *Int. Symp. on Medical Simulation*, pp. 28–37. New York, NY: Springer.
49. Lister K, Gao Z, Desai JP. 2011 Development of *in vivo* constitutive models for liver: application to surgical simulation. *Ann. Biomed. Eng.* **39**, 1060–1073. (doi:10.1007/s10439-010-0227-8)
50. Untaroiu CD, Lu YC, Siripurapu SK, Kemper AR. 2015 Modeling the biomechanical and injury response of human liver parenchyma under tensile loading. *J. Mech. Behav. Biomed. Mater.* **41**, 280–291. (doi:10.1016/j.jmbbm.2014.07.006)
51. Martínez-Martínez F, Lago M, Rupérez M, Monserrat C. 2013 Analysis of several biomechanical models for the simulation of lamb liver behaviour using similarity coefficients from medical images. *Comput. Methods Biomech. Biomed. Eng.* **16**, 747–757. (doi:10.1080/10255842.2011.637492)

52. Capilnasiu A, Bilston L, Sinkus R, Nordsletten D. 2020 Nonlinear viscoelastic constitutive model for bovine liver tissue. *Biomech. Model. Mechanobiol.* **19**, 1–22. (doi:10.1007/s10237-020-01297-5)
53. Gao Z, Lister K, Desai JP. 2010 Constitutive modeling of liver tissue: experiment and theory. *Ann. Biomed. Eng.* **38**, 505–516. (doi:10.1007/s10439-009-9812-0)
54. Umale S, Deck C, Bourdet N, Dhumane P, Soler L, Marescaux J, Willinger R. 2013 Experimental mechanical characterization of abdominal organs: liver, kidney & spleen. *J. Mech. Behav. Biomed. Mater.* **17**, 22–33. (doi:10.1016/j.jmbbm.2012.07.010)
55. Snedeker JG, Niederer P, Schmidlin F, Farshad M, Demetropoulos C, Lee J, Yang K. 2005 Strain-rate dependent material properties of the porcine and human kidney capsule. *J. Biomech.* **38**, 1011–1021. (doi:10.1016/j.jbiomech.2004.05.036)
56. Isvilanonda V, Iaquinto JM, Pai S, Mackenzie-Helnwein P, Ledoux WR. 2016 Hyperelastic compressive mechanical properties of the subcalcaneal soft tissue: an inverse finite element analysis. *J. Biomech.* **49**, 1186–1191. (doi:10.1016/j.jbiomech.2016.03.003)
57. Kwak Y, Kim J, Lee KM, Koo S. 2020 Increase of stiffness in plantar fat tissue in diabetic patients. *J. Biomech.* **107**, 109857. (doi:10.1016/j.jbiomech.2020.109857)
58. Chen WM, Park J, Park SB, Shim VPW, Lee T. 2012 Role of gastrocnemius–soleus muscle in forefoot force transmission at heel rise—a 3D finite element analysis. *J. Biomech.* **45**, 1783–1789. (doi:10.1016/j.jbiomech.2012.04.024)
59. Chokhandre S, Halloran JP, Erdemir A. 2012 A three-dimensional inverse finite element analysis of the heel pad. *J. Biomech. Eng.* **134**, 031002. (doi:10.1115/1.4005692)
60. Erdemir A, Saucerman JJ, Lemmon D, Loppnow B, Turso B, Ulbrecht JS, Cavanagh PR. 2005 Local plantar pressure relief in therapeutic footwear: design guidelines from finite element models. *J. Biomech.* **38**, 1798–1806. (doi:10.1016/j.jbiomech.2004.09.009)
61. Spears I, Miller-Young J, Sharma J, Ker R, Smith F. 2007 The potential influence of the heel counter on internal stress during static standing: a combined finite element and positional MRI investigation. *J. Biomech.* **40**, 2774–2780. (doi:10.1016/j.jbiomech.2007.01.004)
62. Maas SA, Ellis BJ, Ateshian GA, Weiss JA. 2012 FEBio: finite elements for biomechanics. *J. Biomech. Eng.* **134**, 011005. (doi:10.1115/1.4005694)
63. Connolly SJ, Mackenzie D, Gorash Y. 2019 Isotropic hyperelasticity in principal stretches: explicit elasticity tensors and numerical implementation. *Comput. Mech.* **64**, 1273–1288. (doi:10.1007/s00466-019-01707-1)
64. Sugerman GP, Chokshi A, Rausch MK. 2021 Preparation and mounting of whole blood clot samples for mechanical testing. *Curr. Protoc.* **1**, e197. (doi:10.1002/cpz1.197)
65. Blaber J, Adair B, Antoniou A. 2015 Ncorr: open-source 2D digital image correlation Matlab software. *Exp. Mech.* **55**, 1105–1122. (doi:10.1007/s11340-015-0009-1)
66. Weickenmeier J, Mazza E. 2019 Inverse methods. In *Skin Biophysics*, pp. 193–213. New York, NY: Springer.
67. Han T, Lee T, Ledwon J, Vaca E, Turin S, Kearney A, Gosain AK, Tepole AB. 2021 Bayesian calibration of a computational model of tissue expansion based on a porcine animal model. *Acta Biomater.* **137**, 136–146. (doi:10.1016/j.actbio.2021.10.007)
68. Kluyver T *et al.* 2016 Jupyter Notebooks – a publishing format for reproducible computational workflows. In *Positioning and Power in Academic Publishing: Players, Agents and Agendas* (eds F Loizides, B Schmidt), pp. 87–90. Amsterdam, The Netherlands: IOS Press.
69. Virtanen P *et al.* 2020 SciPy 1.0: fundamental algorithms for scientific computing in python. *Nat. Methods* **17**, 261–272. (doi:10.1038/s41592-019-0686-2)
70. Conn AR, Gould NI, Toint PL. 2000 *Trust region methods*. Philadelphia, PA: SIAM.
71. Moerman KM, Simms CK, Nagel T. 2016 Control of tension–compression asymmetry in Ogden hyperelasticity with application to soft tissue modelling. *J. Mech. Behav. Biomed. Mater.* **56**, 218–228. (doi:10.1016/j.jmbbm.2015.11.027)
72. Ehret AE. 2015 On a molecular statistical basis for Ogden’s model of rubber elasticity. *J. Mech. Phys. Solids* **78**, 249–268. (doi:10.1016/j.jmps.2015.02.006)
73. Lohr MJ, Sugerman GP, Kakaletsis S, Lejeune E, Rausch MK. 2022 An introduction to the Ogden model in biomechanics – benefits, implementation tools, and limitations. Figshare. (<https://doi.org/10.6084/m9.figshare.c.6098644>)